Impedance analysis of Al_2O_3/H-terminated diamond metal-oxide-semiconductor structures

Meiyong Liao,[1,2,a)] Jiangwei Liu,[2] Liwen Sang,[3] David Coathup,[1] Jiangling Li, Masataka Imura,[2] Yasuo Koide,[2] Haitao Ye[1,b)]

[1]*School of Engineering and Applied Science, Aston University, Birmingham B4 7ET, United Kingdom*

[2]*Optical and Electronic Materials Unit, National Institute for Materials Science, Namiki 1-1, Tsukuba, Ibaraki 3050044, Japan*

[3]*International Center for Materials Nanoarchitectonics (MANA), National Institute for Materials Science, Namiki 1-1, Tsukuba, Ibaraki 3050044, Japan*

Impedance spectroscopy (IS) analysis is carried out to investigate the electrical properties of the metal-oxide-semiconductor (MOS) structure fabricated on hydrogen-terminated single crystal diamond. The low-temperature atomic layer deposition Al_2O_3 is employed as the insulator in the MOS structure. By numerically analysing the impedance of the MOS structure at various biases, the equivalent circuit of the diamond MOS structure is derived, which is composed of two parallel capacitive and resistance pairs, in series connection with both resistance and inductance. The two capacitive components are resulted from the insulator, the hydrogenated-diamond surface, and their interface. The physical parameters such as the insulator capacitance are obtained, circumventing the series resistance and inductance effect. By comparing the IS and capacitance-voltage measurements, the frequency dispersion of the capacitance-voltage characteristic is discussed.

a) Electronic mail: meiyong.liao@nims.go.jp

b) Electronic mail: h.ye@aston.ac.uk

Diamond is an outstanding semiconductor for high-power and high-frequency electronic applications due to the exceptional properties, such as wide bandgap, high breakdown electric field, outstanding thermal conductivity, and high carrier mobility.[1-3] Recently, encouraging progress, such as high cut-off frequency, has been achieved in diamond field-effect transistors (FETs) by using two-dimensional hole gas based on the p-type hydrogenated-terminated diamond surface.[4-9] Among the diamond FETs, metal-oxide-semiconductor FETs (MOSFETs) have been attracting growing interest because of the higher power handling capability.[10] For example, a high drain current density above 1 A/mm has been reported.[11,12] To further improve the performance of diamond MOSFETs and apply the devices to practical applications, it is critical to obtain the relevant physical parameters such as the gate capacitance and the equivalent circuit of the MOS structure.

The determination of the precise gate capacitance of the MOS structure is crucial for the extraction of the dielectric constant or the thickness of the oxide, carrier mobility, and trap density. Traditional capacitance-voltage (C-V) measurement on MOS structures has the drawback of the influence of imperfect contact and semiconductor series resistance, leading to misinterpretation[13]. Especially, when there is a tunnelling leakage through the gate oxide, the quasistatic capacitance measurement turns to be difficult. In turn, high-frequency measurement should be applied to circumvent the leakage problem so that the capacitive current is dominant.[14] However, in such a case, the effect of the series resistance and shunt parasitic resistance will be pronounced due to the low impedance of the capacitor. Impedance spectroscopy (IS) could avoid the effect of series resistance, thus, offering more reliable capacitance values, particularly for the structure with variable series resistance.[15] On the other hand, the small-signal equivalent circuit can be obtained from the frequency response of the IS measurement. The IS technique has been effectively utilized to analyse the electric transport of bulk diamond and nanodiamonds, previously.[16-19] However, no efforts have been made on the more complex diamond MOS structure.

In this work, the impedance of the MOS structure fabricated on hydrogen-terminated diamond with the atomic layer deposition (ALD)-Al_2O_3 insulator layer was measured and analysed. The equivalent circuit and physical parameters such as the capacitance of the ALD-Al_2O_3 (or dielectric constant) and the series resistance were obtained. The frequency dispersion of the C-V measurement was also discussed in terms of the IS analysis.

The intrinsic homoepitaxial diamond layer with p-type hydrogen-terminated surface for the MOS structure fabrication was deposited on the high-pressure high temperature (HPHT) Ib-type single crystalline diamond (100) substrate (2.6×2.6 mm^2 square) by a microwave plasma chemical vapour deposition technique. The thickness of the diamond epilayer was around 200 nm. A standard photolithographic technique was used for the fabrication of the diamond MOS structure. The Ohmic metal contacts of Au/Ti/Pd (200/20/10 nm: Pd was the first contact to diamond) were deposited by an e-beam evaporation with a base pressure of 10^{-5}Pa.[20] After the lift-off and the second lithography, an ALD-Al_2O_3 layer with a thickness of 25 nm was deposited on the defined circle pattern with diameters of 400 and 500 μm. Afterwards, the Au/Ti electrode was deposited on the Al_2O_3 layer. The interspacing between the Ohmic and the Al_2O_3 insulator was 20 μm. The ALD-Al_2O_3 layer was deposited with a PICOSUN reactor (SUNALE R-100B) under a chamber pressure of 10^3 Pa with precursors of $Al(CH_3)_3$ and water vapour at a substrate temperature of 120 ºC. The pulse and purge times for both the precursors were 0.1 and 4.0 s, respectively. The variation of the Al_2O_3 layer thickness was checked to be within 2% on a 2-inch Si wafer. The schematic view of the metal/Al_2O_3/H-diamond MOS structure is illustrated in Fig. 1 (a).

The MOS structure with a diameter of 500 μm behaves like a Schottky diode with a rectifying ratio less than 100, as revealed by the current-voltage characteristics in Fig. 1(b). Here, the Ohmic contact Au/Ti/Pd was grounded. The leakage current was 10^{-6} A at 1 V (reverse bias) and more than 10^{-5}A at -1 V (forward bias). The large leakage current was possibly due to the tunnelling effect originated from the inhomogeneity of the diamond

surface due to the large device area. The C-V curve displays frequency dispersion at high frequency but keeping almost constant at low frequency from 10 to 100 kHz, as revealed in Fig. 1 (c). Accumulation and depletion regions can be clearly identified at forward and reverse biases, respectively. The dielectric constant calculated from the capacitance at 10 to 100 kHz was around 5.8 and at 1 MHz was unreasonably low (< 3), compared to that deposited at low temperatures.[21]

The IS measurements were performed using a two-probe method in the frequency range of 1 Hz to 1 MHz with an ac amplitude 50 mV under various dc biases. We note that the impedances (Z) of the MOS structures (small diameters) with low leakage current are difficult to measure at reverse biases or small forward biases due to the detection limit of the system. Therefore, effective IS curves can only be obtained for the MOS structure with relatively large leakage current in this work, for example, for the devices with large diameters or for the small devices operated at forward biases. The Cole-Cole plots, Re {Z} *vs* –Im{Z} (termed by Z' *vs* –Z"), of the metal/Al_2O_3/H-diamond MOS structure with a diameter of 500 μm are shown in Fig. 2 with different dc biases. As can be seen, all the spectra exhibit semi-circular shape, revealing that the equivalent circuit of the diamond MOS structure consists of both resistance and capacitance. The size of the semi-circle strongly depends on the applied biases, determining the total impedance. As the reverse bias increases, the semicircle expands along the high impedance direction of the real part, which can be ascribed to the increase of the semiconductor shunt resistance. This is consistent with the extension of the depletion region width as the reverse bias increases. At low frequency, the shunt resistance governs the real part of the impedance. At high frequency, the series resistance effect is dominant. It is noted that the imaginary part of the impedance turns to be negative at high frequency. The negative value of the –Im (Z) suggests the existence of inductance in the circuit. For the MOS structure with a diameter of 400 μm, the IS data can be only obtained at forward biases over -0.2 V, and the similar trend of IS plots with varying bias was observed.

The asymmetrical shape of the impedance spectra implies that the equivalent circuit contains more than one resistance-capacitance (RC) pairs. This is reasonable since the MOS structure contains at least the contributions from the insulator, the hydrogenated diamond surface and their interface. Therefore, the R_xC_x (including the diamond capacitance C_d and possible interface states related capacitance) and the insulator $R_{ox}C_{ox}$, in series connection with a resistance R_s and a parasitic inductance (L), are supposed for the analysis, as shown in Fig. 3(a). The parasitic inductance always appears when the device becomes electrically conductive. The ac impedance of the MOS structure can be expressed as

$$Z(\omega) = Z'(\omega) + jZ"(\omega) \quad (1)$$

where ω is the angular frequency, Z' and $Z"$ are the magnitudes of the real and imaginary parts of the impedance, respectively.

$$Z' = \frac{R_{ox}}{1+(\omega R_{ox}C_{ox})^2} + \frac{R_X}{1+(\omega R_X C_X)^2} + R_s \quad (2)$$

$$Z" = -\frac{\omega R_{ox}^2 C_{ox}}{1+(\omega R_{ox}C_{ox})^2} - \frac{\omega R_X^2 C_X}{1+(\omega R_X C_X)^2} + \omega L \quad (3)$$

where ω is the angular frequency. The experimental Cole-Cole plots of Fig. 2 were well fitted by the equivalent circuit shown in Fig. 3 (a) for the MOS structures with different diameters at varying dc biases. The series resistance is less than 1 kΩ, which originates from the electric contact and the semiconductor diamond. The resulting capacitances C_{ox} of the insulator are around 650 pF and 350 pF for the devices with 500 and 400 μm diameters, respectively. As displayed in Fig.4, the resultant C_{ox} varies little with the applied biases, supporting the validity of the numerical fitting. If the capacitance C_{ox} is only from the Al_2O_3 insulator, the dielectric constant of the ALD-Al_2O_3 layer was estimated to be around 7.5-9.5. This value is close to those documented previously.[22,23] However, the derived capacitance and

corresponding dielectric constant are significantly larger than those obtained by C-V method. On the other hand, the capacitance of C_X (order of 20 pF) increased with increasing the forward bias, which was possibly a series connection of the diamond capacitance C_d with an interface capacitance C_i, shown in Fig. 3 (a). The C_i is likely the capacitance from the interface states, judged from the plateau between the accumulation and depletion regions in the C-V curves in Fig. 1. However, we note that C_i does not affect the fitting of the accumulation capacitance. The details on this capacitance C_i will be investigated later.

In order to interpret the large discrepancy of the capacitance in the accumulation region between the C-V and IS measurement, the IS curves were fitted with different models. As revealed by Fig. 1, the C-V characteristics exhibit frequency dispersion in the accumulation region. Based on this fact, we analysed the impedance by adding a constant phase element (CPE) either in the semiconductor or in the insulator or between them. The frequency dependent impedance of the CPE is defined as [24]

$$Z_{CPE} = \frac{1}{Y_0(j\omega)^n} \quad (4)$$

where Y_0 is the capacitance and resistor, when n=1 and 0, respectively. It was found that the extraction of the reasonable physical parameters was difficult. Therefore, the capacitance in the accumulation region is not related to the direct frequency-dependent CPE.

The capacitance inconsistence between the C-V and IS data possibly results from frequency dispersion in the C-V measurement. Various mechanisms have been put forward to account for the frequency dispersion of the capacitance in the accumulation region, including both extrinsic effect (i.e. series resistance and interface states) and intrinsic effect (i.e. dielectric relaxation). The dielectric relaxation, which actually occurs at wide frequency range (1-10MHz), is unlikely the mechanism for the high-frequency dispersion of the resultant ALD-Al_2O_3 layer.[25] The interface layer between the semiconductor and the insulator, acting as an additional RC pair, in series connection with the insulator and semiconductor RC pairs,

was proposed to analyse the impedance spectra.[26] This, however, did not offer the valid physics parameters in the diamond MOS structure here.

When series resistance was taken as the dominant factor in the C-V measurement, the frequency dependent capacitance can be fitted by the following equation.[27]

$$C_m = \frac{C_i}{(1+R_sG)^2+(R_s\omega C_i)^2} \quad (5)$$

where C_m is the measured capacitance and G is the conductance of the insulator. According to the fitting, the effective dielectric constant was corrected to be 7.3, similar to that obtained by the IS analysis. Therefore, the series resistance is considered as the dominant factor in determining the frequency dispersion in the C-V measurement, and the IS provides an effective tool to characterize the MOS structure.

The validity of the IS technique was verified by measuring the impedance of a metal/Al_2O_3/H-diamond MOS structure with high resistivity at reverse biases, as shown in Fig. 5. The leakage current at reverse bias was much lower than that in Fig. 1, as displayed in Fig.S2, and the capacitance measured at reverse bias showed little dependence on frequency (Fig. S3).[28] Therefore, we employed an equivalent circuit (inset in Fig. 5 (b)) similar to that for the C-V measurement to fit the IS data in Fig. 5 (a). As a result, the derived capacitance from the IS data is almost the same as that measured by the C-V technique. Similar to the device in Fig. 1, the capacitance in the accumulation region for this high-resistance device showed frequency dispersion (Fig.S3) at forward biases. Similar to Fig. 4, the extracted capacitance from the IS data was around 1.2 times higher than that measured by the C-V technique (Fig. S4).[28] Therefore, impedance spectroscopy techniques can be used to evaluate the hydrogen-terminated diamond MOS structures of any quality. It can also be applied to MOS structures based on oxygen-terminated diamond surface doped with boron.[3] When the MOS structure has a large leakage current due to the inhomogeneity of the semiconductor surface, the precise measurement of the accumulation capacitance in C-V has to be carried out

at high frequencies. In such a case, the series resistance will affect the capacitance in the C-V measurement. The measurements for the MOS structure in Fig. 1 were performed with either large areas or at forward biases, and the capacitance measured by impedance spectroscopy was not affected by the leakage current. This is because that the leakage current is resulted from the diamond surface rather than the insulator. This approach is thus superior to or a complementary to the conventional C-V measurement. For a device with large resistivity, one can increase the device area or decrease the insulator thickness to increase the signal amplitude to satisfy the limitation of the impedance spectroscopy setup. The other advantage of using the impedance spectroscopy technique over the C-V measurement is to evaluate the interfacial states at the oxide/semiconductor interface. In C-V measurement, the interface or border states are likely to induce frequency dispersion of capacitance.[29] As discussed in this paper, the frequency dispersion of capacitance can also be introduced by series resistance, which will result in inaccuracy during the C-V measurement. However, the interface or border states can be treated as a frequency-dependent constant phase element (CPE) in impedance spectroscopy analysis using equivalent circuits. This therefore provides an effective and straight forward method to identify and evaluate the origin of the frequency dispersion of the capacitance.

In summary, the impedance spectroscopy was employed for the characterization of the diamond MOS structures at various biases. It was revealed from the IS curves that the equivalent circuit contained two RC pairs originated from the insulator, semiconductor, and the insulator/semiconductor interface, in series connecting both resistance and inductance. The IS measurement was able to circumvent the series resistance effect, thus generating more reliable physical parameters. The capacitance of the insulator was extracted from the Cole-Cole plots and the dielectric constant of the insulator was obtained. After correcting the capacitance in the C-V characteristics by the series resistance, the dielectric constant for both

IS and C-V measurements were similar. The IS method provides an effective strategy to obtain not only the equivalent circuit but also the capacitance of the MOS structure.

ACKNOWLEDGEMENTS

This work was supported by FP7 Marie Curie Action (project No: 300193 and 295208) sponsored by European Commission, UK Engineering and Physical Science Research Council (EP/K003070/1), Green Network of Excellence (GRENE), Low-Carbon Research Network (LCnet), and Nanotechnology Platform projects sponsored by the Ministry of Education, Culture, Sports, and Technology (MEXT) in Japan.

References

[1]J. W. Pomeroy,M. Bernardoni, D. C. Dumka, D. M. Fanning, and M. Kuball, Appl. Phys. Lett **104**, 083513 (2014).

[2]S. A. O. Russell, L. Cao, D. Qi, A. Tallaire, K. G. Crawford, A. T. S. Wee, and D. A. J. Moran, Appl. Phys. Lett. **103**, 202112 (2013)

[3]G. Chicot, A. Marechal, R. Motte, P. Muret, E. Gheeraert, and J. Pernot, Appl. Phys. Lett, **102**, 242108 (2013).

[4]K. Ueda, K. M. Kasu, Y.Yamauchi, T. Makimoto, M. Schwitters, D. J. Twitchen, G.A. Scarsbrook, S. E. Coe, IEEE Elec. Dev. Lett. **27**, 570 (2006).

[5]C. Pietzka ,J. Scharpf,M. Fikry, D. Heinz, K. Forghani,T. Meisch,Th. Diemant,R. J. Behm,J. Bernhard,J. Biskupek,U. Kaiser,F. Scholz and E. Kohn, J. Appl. Phys. 114, 114503 (2013).

[6]M. Kubovic, M.Kasu, Appl. Phys. Exp**. 2**, 086502 (2009).

[7]M. Kasu, K. Ueda, H. Ye, Y. Yamauchi, N. Maeda, S. Sasaki and T. Makimoto, IEE Electronics Letters **41,** 22 (2005).

[8]Kasu, K. Ueda, H. Ye, Y. Yamauchi, S. Sasaki, and T. Makimoto, Diamond and Related Materials **15**, 783(2006).

[9]H. Ye, M. Kasu, Y. Yamauchi, N. Maeda, S. Sasaki and T. Makimoto, Diamond and Related Materials **15**,787 (2006).

[10]S.H. Cheng, L. W. Sang, M. Y. Liaom J. W. Liu, M. Imura, H. D. Li, Y. Koide, Appl. Phys. Lett. **101**, 202907 (2012).

[11]K. Hirama, H. Sato, Y. Harada, H. Yamamoto, and M. Kasu, J. J. Appl. Phys**. 51**, 090112 (2012).

[12]H. Kawarada, J. J. Appl. Phys. **51**, 090111 (2012).

[13]B. Yao, Z. B. Fang,Y. Y. Zhu, T. Ji, and G. He, Appl. Phys. Lett. **100**, 222903 (2012).

[14]K. J. Yang, C. Hu, IEEE Trans. Electron. Dev. **46**, 1500 (1999).

[15]C. Yim, N. McEvoy, and G. S. Duesberg, Appl. Phys. Lett. **103**, 193106 (2013).

[16] N. Tumilty ,J. Welch, H. Ye, R.S. Balmer, C. Wort, R.Lang, and R. B. Jackman, Appl. Phys. Lett, **94**, 052107 (2009).

[17]H. Ye, C. Sun, H. Huang and P. Hing, App. Phy.Lett. **78**,1826 (2001).

[18]S. Curat, H. Ye, O. Gaudin, R. Jackman and S. Koizomi, J. Appl.Phys. **98,** 073701 (2005).

[19]S. Su, J. Li, V. Kundrát, A.M. Abbot, H. Ye, J. Appl. Phy. **11**.3023707 (2013).

[20] J .W. Liu, M. Y. Liao, *Scientific Reports* **4**,6395 (2014).[21]M. D. Groner, F. H. Fabreguette, J. W. Elam, and S. M. George, Chem. Mater. **16**, 639 (2004)

[22]S. K. Kim, S. W. Lee, C. S. Hwang, Y.S. Min, J. Y. Won, and J. Jeong, J. Electrochemical Soc. **153**, F69 (2006).

[23]C. M. Tanner, Y. C. Perng, C. Frewin and S. E. Saddow, J. P. Chang, Appl. Phys. Lett. **91**, 203510 (2007).

[24]M. Donahue, B. Lubbers, M. Kittler, P. Mai, and A. Schober, Appl. Phys. Lett. **102**, 141607 (2013).

[25]C. Zhao, C. Z. Zhao, M. Werner, S. Taylor and P. Chalker, Nano. Res. Lett. **8**, 456 (2013).

[26]X. Li, Y. Cao, D. C. Hall, P. Fay, X. Zhang and R. D. Dupuis, J. Appl. Phys. **95**, 4209 (2004).

[27]D. K. Schroder, Semiconductor Material and Device characterization, Wiley, New York, 1998.

[28] See supplementary material at http://dx.doi.org/10.1063/1.4913597 for the information of the uniformity of the ALD-Al2O3 layer and the impedance spectra of the MOS structure with high resistivity.

[29] K. Takei, R. Kapadia, H. Fang, E. Plis, S. Krishna, A. Javey, Appl. Phys. Lett. **102**, 153513 (2013).

Figure Captions

FIG.1. (a) Metal-oxide-semiconductor structure based on hydrogenated diamond surface, (b) current-voltage characteristics of the diamond MOS structure, and (c) capacitance-voltage characteristics at different frequencies.

FIG. 2. Impedance spectra of the diamond MOS structure measured at different biases in the frequency range of 1Hz to 1MHz**.**

FIG.3. (a) Equivalent circuit of the diamond MOS structure, (b)-(e) numerical analysis of the impedance spectra based on the equivalent circuit**.**

FIG.4. Derived capacitance of the ALD-Al_2O_3 from the impedance spectra for the diamond MOS structures with diameters of 400 and 500 μm.

FIG.5 (a) Impedance spectra of MOS structure based on hydrogen terminated diamond with high resistivity at reverse biases, (b) derived capacitance from the IS data by using the equivalent circuit inserted.

Figure 1

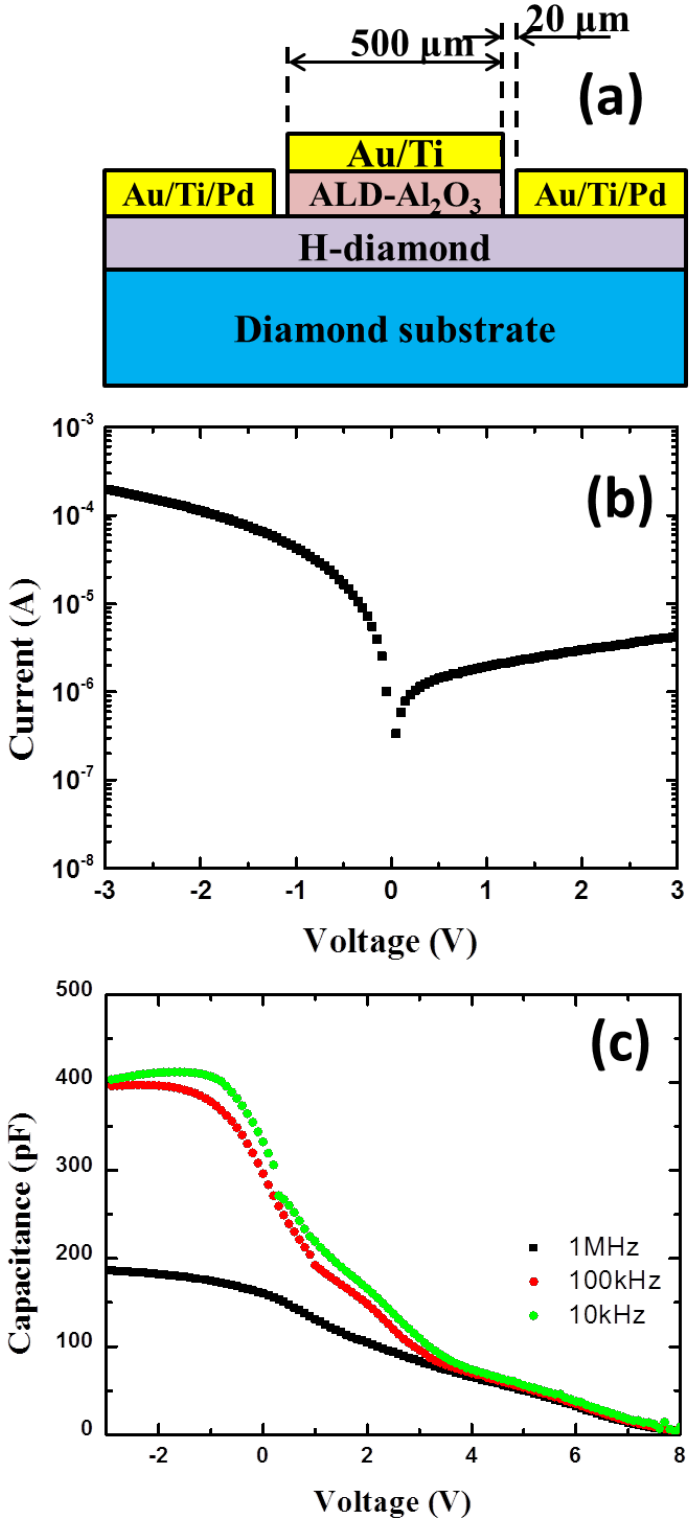
20 µm
500 µm
(a)
Au/Ti
Au/Ti/Pd
ALD-Al2O3
Au/Ti/Pd
H-diamond
Diamond substrate
(b)
Current (A)
Voltage (V)
(c)
Capacitance (pF)
1MHz
100kHz
10kHz
Voltage (V)

Figure 2

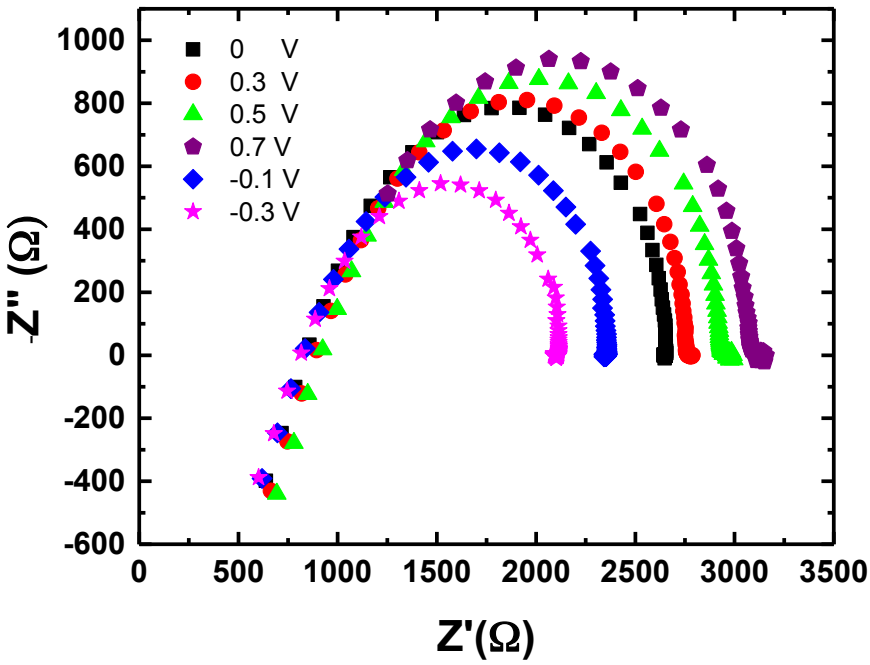
0 V
0.3 V
0.5 V
0.7 V
-0.1 V
-0.3 V
Z'' (Ω)
Z'(Ω)
1000
800
600
400
200
0
-200
-400
-600
0
500
1000
1500
2000
2500
3000
3500

Figure 3

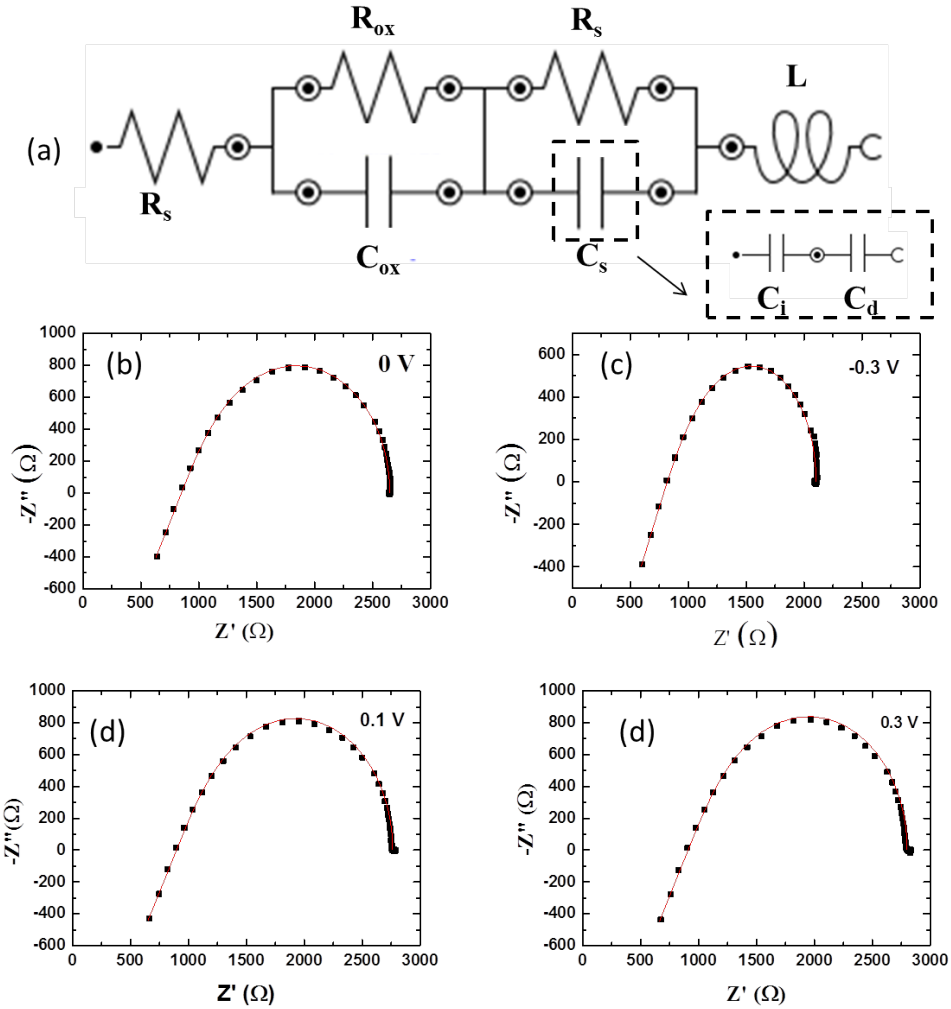

Figure 4

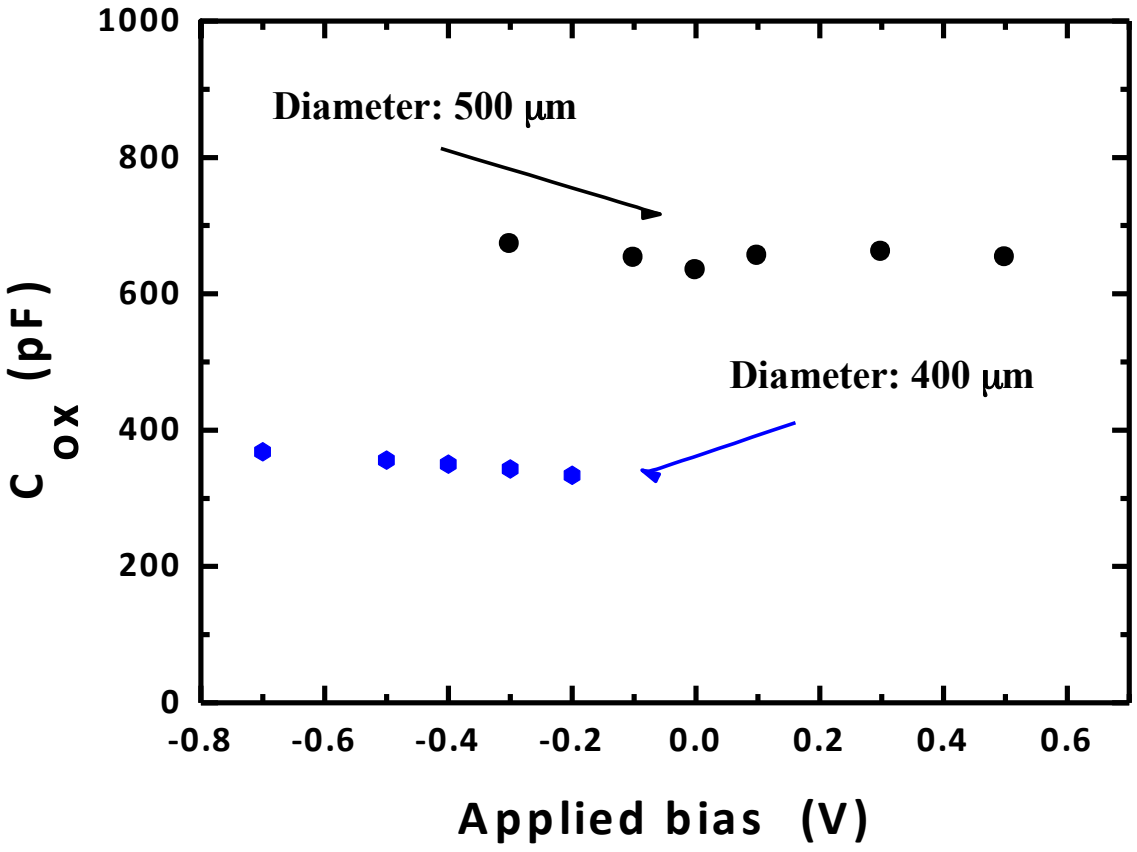
1000
800
600
400
200
0
C ox (pF)
Diameter: 500 μm
Diameter: 400 μm
-0.8
-0.6
-0.4
-0.2
0.0
0.2
0.4
0.6
Applied bias (V)

Figure 5

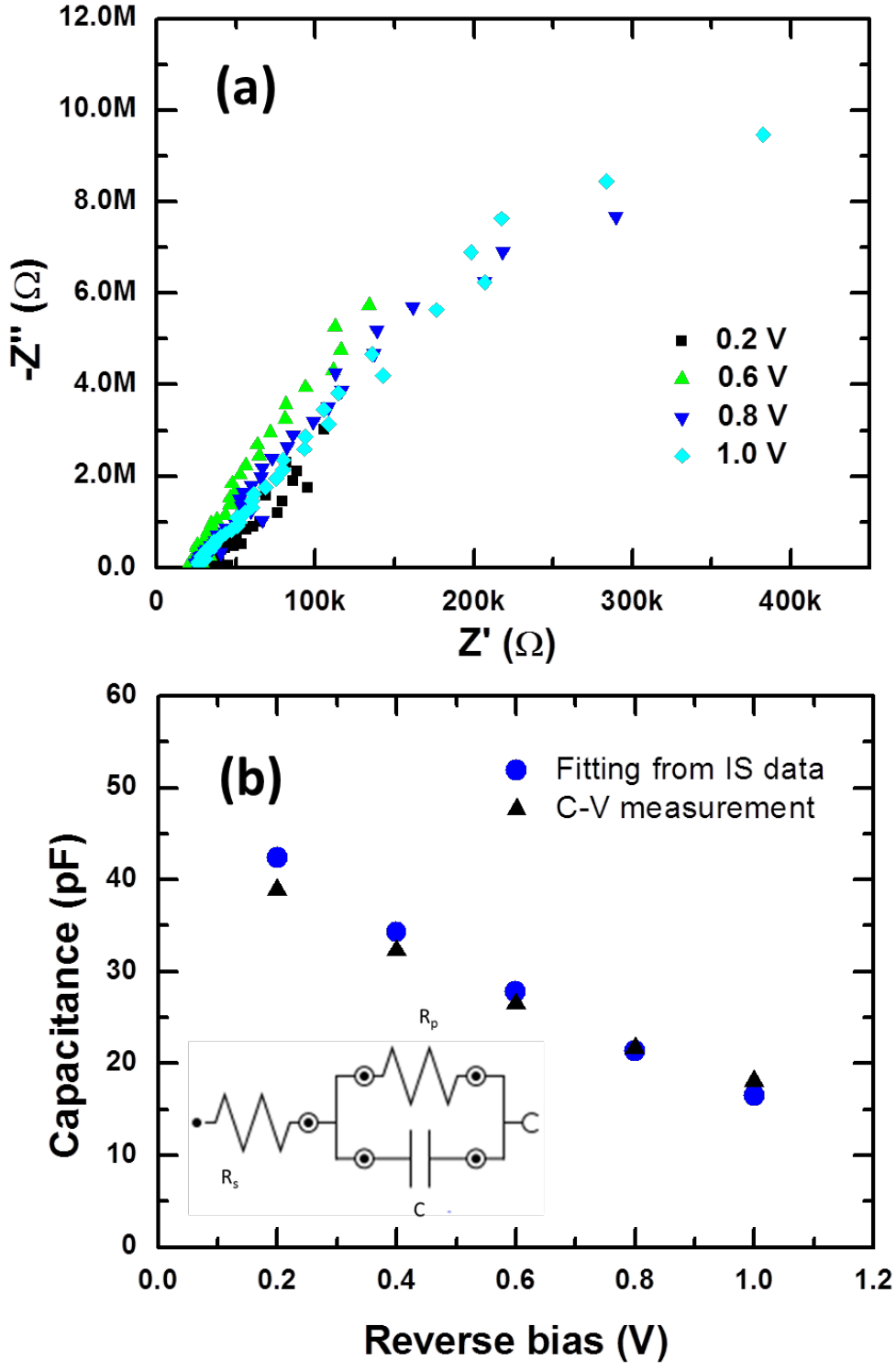
(a)
12.0M
10.0M
8.0M
6.0M
4.0M
2.0M
0.0
-Z'' (Ω)
0
100k
200k
300k
400k
Z' (Ω)
0.2 V
0.6 V
0.8 V
1.0 V
(b)
Fitting from IS data
C-V measurement
Capacitance (pF)
60
50
40
30
20
10
0
0.0
0.2
0.4
0.6
0.8
1.0
1.2
Reverse bias (V)
Rp
Rs
C
C